Human TRAF3 adaptor molecule deficiency leads to impaired Toll-like receptor 3 response and susceptibility to herpes simplex encephalitis

Rebeca Pérez de Diego [1,2,3], Vanessa Sancho-Shimizu[1,2,3], Lazaro Lorenzo [1,2,3], Anne Puel[1,2,3], Sabine Plancoulaine[1,2,3], Capucine Picard[1,2,4], Melina Herman[1,2,3], Annabelle Cardon[1,2,3], Anne Durandy[4], Jacinta Bustamante[1,2,3], Sivakumar Vallabhapurapu[5], Jerónimo Bravo[6], Klaus Warnatz[7], Yves Chaix[8], Françoise Cascarrigny[9], Pierre Lebon[10], Flore Rozenberg[10], Michael Karin[5], Marc Tardieu[11], Saleh Al-Muhsen[12], Emmanuelle Jouanguy[1,2,3], Shen-Ying Zhang[1,2,3], Laurent Abel[1,2,3] and Jean-Laurent Casanova[1,2,3,12,13]*

[1]Laboratory of Human Genetics of Infectious Diseases, Necker Branch, INSERM U550, Necker Medical School, Paris 75015, France, EU.
[2]University Paris Descartes, Paris 75015, France, EU.
[3] St. Giles Laboratory of Human Genetics of Infectious Diseases, Rockefeller Branch, The Rockefeller University, New York, NY 10065, USA.
[4]Study Center of Primary Immunodeficiencies, Necker Hospital, AP-HP, Paris 75015, France, EU.
[5]Laboratory of Gene Regulation and Signal Transduction, Departments of Pharmacology and Pathology, Cancer Center, University of California, San Diego, California 93093, USA.
[6]Signal Transduction Unit. Instituto de Biomedicina de Valencia (IBV-CSIC), Valencia 46010, Spain, EU.
[7]Division of Rheumatology and Clinical Immunology, University Clinic Freiburg, Freiburg 79106, Germany, EU.
[8]Pediatric Neurology, Toulouse Hospital, Toulouse 31059, France, EU.
[9]Pediatric service, Montauban Hospital, Montauban 82013, France, EU.
[10]Virology, Cochin-Saint-Vincent de Paul Hospital, University Paris René Descartes, Paris 75014, France, EU.
[11]Pediatric Neurology, Bicêtre Hospital, University Paris Sud, Kremlin-Bicêtre 94270, France, EU.
[12]Novel primary immunodeficency and infectious diseases program, Department of Pediatrics, College of Medicine, King Saud University, Riyadh 11451, Saudi Arabia.
[13]Pediatric Hematology-Immunology Unit, Necker Hospital, Paris 75015, France, EU.

***Corresponding author:** Jean-Laurent Casanova
jean-laurent.casanova@inserm.fr
jean-laurent.casanova@rockefeller.edu
Voice 1 212 327 7331
Fax 1 212 327 7330

Keywords: Herpes simplex encephalitis (HSE), TRAF3, herpes simplex virus 1 (HSV-1), TLR3, interferon (IFN).

Running title: Human TRAF3 deficiency

ABSTRACT

Tumor necrosis factor (TNF) receptor-associated factor 3 (TRAF3) functions downstream of multiple TNF receptors and other receptors which induce interferon-α (IFN-α), IFN–β and IFN-λ production, including TLR3 which is deficient in some patients with herpes simplex virus-1 (HSV-1) encephalitis (HSE). Mice lacking TRAF3 die in the neonatal period, preventing direct investigation of the role of TRAF3 in immune responses and host defenses *in vivo*. Here we report autosomal dominant, human TRAF3 deficiency in a young adult with a history of HSE in childhood. The *TRAF3* mutant allele is loss-of-expression, loss-of-function, dominant-negative, and associated with impaired, but not abolished TRAF3-dependent responses upon stimulation of both TNF receptors and receptors which induce IFN production. Nevertheless, TRAF3 deficiency is associated with a clinical phenotype limited to HSE and resulting from the impairment of TLR3-dependent induction of IFN-α/β and –λ. Thus, TLR3-mediated immunity against primary infection by HSV-1 in the central nervous system is critically dependent on TRAF3.

Highlight sentence: Autosomal dominant TRAF3 deficiency is a genetic etiology of herpes simplex encephalitis.

Highlight sentence: The R118W TRAF3 allele is loss-of-function, loss-of-expression, and dominant-negative.

Highlight sentence: Human TRAF3 deficiency impairs the TLR3-dependent induction of anti-viral interferons.

INTRODUCTION

Herpes simplex virus (HSV-1) encephalitis (HSE) is a devastating infection of the central nervous system (CNS) (Whitley, 2006). HSE is the most common form of sporadic viral encephalitis in Western countries, in which its incidence has been estimated at approximately 1 in 250,000 individuals per year. The disease peaks in childhood, between the ages of three months and six years. During primary infection with HSV-1, the virus reaches the CNS via a neurotropic route involving the trigeminal and olfactory nerves (Abel et al.; De Tiege et al., 2008). Acyclovir treatment decreases the mortality rate in affected children, but substantial neurological impairment is nevertheless observed in most survivors, and in particular, in young children. However, HSV-1 is widespread and typically innocuous in human populations.

Childhood HSE was not associated with known immunodeficiencies and the mechanism of its pathogenesis remained elusive until we identified the first two genetic etiologies of this condition: autosomal recessive UNC-93B deficiency, which abolishes Toll-like receptor 3 (TLR3), TLR7, TLR8, and TLR9 signaling (Casrouge et al., 2006), and autosomal dominant TLR3 deficiency, which specifically affects TLR3 signaling (Zhang et al., 2007). These findings are consistent with the lack of HSE in patients with IRAK-4 and MyD88 deficiencies, as these patients have a functional TLR3, but non functional TLR7, TLR8, and TLR9 (Picard et al., 2003; von Bernuth et al., 2008; Yang et al., 2005)

Our previous demonstration that STAT1 deficiency, unlike IFN-γR1 or IFN-γR2 deficiency, confers predisposition to multiple viral diseases, including HSE, suggested that impairment of the TLR3-dependent production of IFN-α and IFN-β (type I IFN) and IFN-λ (type III IFN) might account for HSE in patients with TLR3 and UNC-93B deficiencies (Chapgier et al., 2009; Dupuis et al., 2003). Collectively, these studies

suggest that childhood HSE may result from impaired type I and/or type III IFN production in response to the stimulation of TLR3 by dsRNA intermediates of HSV-1 in the CNS, in at least some children. As only a small fraction of children with HSE carry mutations in the TLR3 and UNC-93B genes, we searched for mutations in other genes controlling the TLR3 pathway. Here, we report on an autosomal dominant deficiency of the TRAF3 adaptor protein in a patient with HSE. This experiment of Nature indicates that TLR3-mediated immunity against primary infection by HSV-1 in the central nervous system is critically dependent on TRAF3.

RESULTS

Heterozygous *TRAF3* mutation in a patient with HSE

We investigated an 18-year-old French girl (P1) who had suffered from HSE at the age of four years (Supplemental data text, note 1) and carried no mutation in the coding region of *UNC93B1* or *TLR3*, the mRNAs of which were normally spliced and generated in normal amounts. No mutations were found in the coding regions of seven other genes known to control the TLR3 – type I IFN pathway, encoding Toll-IL-1 receptor domain-containing adaptor protein-inducing IFN-β (TRIF), TRAF-interacting protein I-TRAF (TANK), the adaptor protein SINTBAD, NAK-associated protein-1 (NAP1), TANK-binding kinase 1 (TBK1), Iκ-B kinase-ε (IKK-ε), and the transcription factor IRF-3. A heterozygous substitution (C→T) was found at nucleotide position 352 (c.352C>T) in exon 4 of the gene encoding TNF receptor-associated factor 3 (*TRAF3)* (Bishop and Xie, 2007; Hacker et al., 2006; He et al., 2007; Oganesyan et al., 2006) in genomic DNA (gDNA) from the granulocytes, EBV-transformed B cells (EBV-B cells), and SV40-transformed fibroblasts (SV40-fibroblasts) of P1 (Fig. 1A and B). No other mutations were found in the coding region of *TRAF3*. The *TRAF3* mutation is missense and non conservative, as it replaces an Arg residue at position 118 in the first of the five zinc-finger domains with a Trp residue (R118W) (Fig. 1C). R118W was not found in the NCBI and Ensembl databases or in up to 1,209 unrelated healthy individuals (2,418 chromosomes) from the CEPH-Human Genome Diversity panel examined, including 289 Europeans, ruling out an irrelevant polymorphism. The father, mother and brothers of P1 do not carry the R118W mutation. Alignment of the human *TRAF3* sequence with sequences from the 13 animal species in which *TRAF3* has been sequenced showed R118 to be strictly conserved throughout evolution (Fig. S1). These data suggest that

the *de novo* R118W germline mutation in *TRAF3* may be responsible for the autosomal dominant predisposition to HSE in P1.

Impaired TRAF3 production in cells from the patient

We then assessed the expression of TRAF3 mRNA and protein in cells from P1. Quantitative PCR showed baseline TRAF3 mRNA expression in SV40-fibroblasts (human fibroblasts immortalized with SV40) (Fig. 2A) and EBV-B cells (human B cells immortalized with EBV) (Fig. S2A) from P1 to be normal. The wild-type (WT) and mutant *TRAF3* alleles were expressed to similar extents, as shown by direct sequencing of the RT-PCR product (data not shown). In contrast, TRAF3 protein in SV40-fibroblasts (Fig. 2A) and EBV-B cells (Fig. S2B) from P1 were only about 17.5% those in five unrelated healthy controls (data not shown), as shown by immunoblot analysis. Similar results were obtained with two additional antibodies recognizing different TRAF3 epitopes at some distance from residue 118 (Fig. S2C). The R118W mutation therefore seems to prevent stable TRAF3 protein production. It also seems to have an effect on the amount of WT protein generated from the other allele. We stably transfected a TRAF3-knockdown RAW mouse macrophage cell line (RAW *Traf3*$^{-/-}$) (Tseng et al., 2010) with vectors encoding the WT or R118W human *TRAF3* allele. TRAF3 protein was detected after transfection with the WT construct, but not after transfection with the mock vector or the R118W allele, whereas mRNA was detected for both the WT and R118W forms (Fig. 2B).

Impaired TLR3 responsiveness of the patient's fibroblasts

The induction of IFN-β and, subsequently, of IFN-inducible target genes in response to TLR3 agonists is markedly impaired in bone marrow-derived macrophages

(BMMs) generated from irradiated C57BL/6 mice, reconstituted with Traf3$^{-/-}$ fetal liver cells (Hacker et al., 2006; Oganesyan et al., 2006). We investigated the contribution of TRAF3 deficiency to the pathogenesis of HSE in P1, by evaluating the TLR3 pathway in SV40-transformed dermal fibroblasts, in which the response to poly(I:C) is TLR3-dependent (Casrouge et al., 2006; Zhang et al., 2007). In control SV40-fibroblasts, IFN-β, IFN-λ and IL-6 were secreted in a time- and dose-dependent manner, after TLR3 stimulation with poly(I:C) (Fig. 2C). In contrast, cells from P1 and from an UNC-93B-deficient patient did not respond. TNF-α-induced IL-6 production was normal, indicating that the differences in IFN-β, IFN-λ and IL-6 production upon TLR3 stimulation were not due to a general non-responsiveness of the cells (Fig. S2D). Similar results were obtained for the IFN-β and IFN-λ mRNAs (Fig. S2E) and for analyses of primary dermal fibroblasts (data not shown).

We dissected the cellular phenotype of P1 further, by studying two transcription factors controlling the TLR3-IFN pathway: NF-κB and IRF-3. Accumulation of the NF-κB p65 subunit in the nucleus in response to poly(I:C) was impaired in P1, as shown by ELISA (Fig. 2D), whereas the response to both TNF-α and IL-1β was normal. In contrast, the dimerization of IRF-3 in response to poly(I:C) in SV40-fibroblasts from P1 was less strongly affected, as shown by comparisons with healthy controls and with TLR3-deficient and UNC-93B-deficient cells (Fig. 2E) (Casrouge et al., 2006; Zhang et al., 2007). The TRAF3 deficiency therefore affected the TLR3 pathway, in terms of the activation of NF-κB and, to a lesser extent, IRF-3. This resulted in the impairment of cytokine production, with the abolition of IFN-β, IFN-λ and IL-6 induction by poly(I:C), in particular.

Complementation of the patient's cells with wild-type TRAF3

P1 fibroblasts were transfected with WT *TRAF3* and stable transfectants were obtained (Fig. 3A). These cells contained no more than about 30% the amount of TRAF3 present in healthy controls. However, they contained more TRAF3 than non transfected and mock-transfected P1 cells, which contained only about 17.5% the amount of TRAF3 present in controls (Fig. 3A), consistent with the mutant allele being structurally dominant-negative. Nevertheless, stable transfection with the WT *TRAF3* allele, unlike mock transfection, complemented the defect in the TLR3-dependent induction of IFN-β, IL-6 (Fig. 3B) and IFN-λ (Fig. S3A), indicating that the doubling of TRAF3 amounts, although modest, was sufficient to overcome the functional defect. No complementation of the phenotype was observed after transfection with R118W *TRAF3* (Figures S3B and S3C). Thus, the WT *TRAF3* allele complemented the lack of response to TLR3 in P1 fibroblasts, strongly suggesting that the patient's fibroblastic phenotype and, by inference from TLR3 and UNC-93B deficiencies (Casrouge et al., 2006; Zhang et al., 2007), the patient's clinical phenotype of HSE, resulted from TRAF3 deficiency.

The *TRAF3* mutant allele is dominant-negative

The WT *TRAF3* allele conferred functional complementation of cells from P1, but TRAF3 protein levels remained lower (~30%) than those in the cells of all healthy controls tested. This finding is consistent with the much lower than expected amounts of TRAF3 in the heterozygous cells of P1 (~ 17.5%). Thus, although the R118W allele is a loss-of-expression allele, it may exert a dominant-negative effect, by destabilizing proteins produced from the WT allele. Mouse RAW macrophages were used to test this hypothesis, because human and mouse TRAF3 proteins are 97% identical and the antibodies recognizing human TRAF3 also recognize its mouse ortholog. The amounts of mouse TRAF3 in RAW cells stably transfected with human R118W *TRAF3* were

only about 50% those in non transfected RAW cells, mock-transfected cells or cells transfected with human WT TRAF3 (Fig. 3C). Similar results were obtained in transient transfection experiments (data not shown). However, this had no functional consequences, as IFN-β production after stimulation with poly(I:C) was normal, implying that the small amount of protein produced was nonetheless sufficient to activate the TLR3 pathway (Fig. 3D), a finding consistent with the successful complementation of the patient's cells by only about 30% the amount of WT human TRAF3 generally found in normal cells (Fig. 3A). Similar results were obtained when SV40-fibroblasts were stably transfected with the same vectors (Fig. S3D and S3E). Moreover transient transfections of RAW *Traf3*$^{-/-}$ cells showed the R118W mutant form to have a dominant-negative effect. In cells co-transfected with a 1:1 ratio of WT *TRAF3* and mock vector or R118W *TRAF3*, we found that TRAF3 protein expression was 30% lower in the presence of the mutant form (Fig. S4A). The co-transfection of cells with different ratios of WT:R118W *TRAF3* showed that TRAF3 protein expression decreased as the proportion of the mutant form increased (Fig. S4A) Moreover, co-transfection with a fixed amount of WT *TRAF3* and increasing amounts of mutant *TRAF3* confirmed the negative dominance by revealing a dose-dependent impact of the mutant allele, in terms of TRAF3 expression (Fig. S4A).

We further investigated the possible effect of the mutant form on the stability of trimer formation, by generating TRAF3 deletion constructs without the C-terminal region implicated in trimer assembly. The deletion of this region from both the WT and R118W forms had no effect on TRAF3 expression in RAW *Traf3*$^{-/-}$ cells co-transfected with the wild-type and deletion constructs (Fig. S4A). Similar results were obtained after the co-transfection of cells with the WT construct and other shorter deletions of *TRAF3* (data not shown). The dominant-negative effect of the R118W allele probably

resulted from the inhibition of TRAF3 trimer formation (Pullen et al., 1999), as the patient's TRAF3 expression (17.5%) was close to the expected frequency of homotrimers composed of WT subunits only (12.5%) (Fig. S4B). Unstable heterotrimers may be more susceptible to protein degradation, resulting in the persistence within cells of only the remaining stable homotrimers. Thus, the R118W *TRAF3* allele exerts a dominant-negative effect in various types of mouse and human cells, by decreasing production of the WT protein, thus accounting for the much lower total amount of TRAF3 present and the profound impairment of TLR3 responses in cells from this heterozygous patient.

Impaired IFN-dependent control of viruses in TRAF3-deficient fibroblasts

We studied fibroblast responses to vesicular stomatitis virus (VSV) infection, which have been shown to be impaired in UNC-93B-deficient and TLR3-deficient patients (Casrouge et al., 2006; Zhang et al., 2007). IFN-β, IFN-λ and IL-6 were produced in smaller amounts by P1 and UNC-93B-deficient SV40-fibroblasts than by control cells (Fig. 4A). The survival of the patient's SV40-fibroblasts was found to be markedly lower than that of control cells, after 24 hours of VSV infection (Fig. 4B). P1 cells behaved like the cells of patients with TLR3, UNC-93B and STAT1 deficiencies (Casrouge et al., 2006; Chapgier et al., 2009; Zhang et al., 2007). Treatment with exogenous IFN-α2b complemented the phenotype of TRAF3-deficient, TLR3-deficient and UNC-93B-deficient cells, but not that of STAT1-deficient cells (Fig. 4B). We also showed that control cells contain VSV replication, whereas cells from P1 and from patients with STAT1, UNC-93B and TLR3 deficiencies did not (Fig. 4C). When cells from P1, UNC-93B-deficient and TLR3-deficient patients were subjected to prior treatment with IFN-α2b, complementation was observed, as viral replication was

contained; no such complementation was observed for STAT1-deficient cells (Fig. 4C). Finally, we attempted to complement the TRAF3 deficiency in these assays of cytokine production, viral replication, and cell death. The production of IFN-β, IFN-λ and IL-6, cell survival and viral replication in response to viral infection were restored in P1 cells stably transfected with the WT construct, but not in cells transfected with the mutant human *TRAF3* allele or the mock vector (Fig. 4D-F , S3A and S3C). Thus, P1 cells display impaired IFN-β production in response to VSV infection, resulting in higher viral replication and cell death, and this phenotype, which is also common to UNC-93B-deficient and TLR3-deficient cells, results from TRAF3 deficiency. These findings identify TRAF3 deficiency as a genetic etiology of HSE, causing disruption of the TLR3-dependent induction of anti-viral type I IFN and IFN-λ.

Impact of TRAF3 deficiency on other IFN-inducing pathways

We also analyzed the impact of TRAF3 deficiency on other pathways, starting with the anti-viral pathways inducing type I IFN and IFN–λ (Bishop and Xie, 2007; He et al., 2007). Previous studies established a role for TRAF3 in the TLR4, TLR7-TLR8 (Hacker et al., 2006; Hoebe and Beutler, 2006; Oganesyan et al., 2006) and RIG-I and MDA-5 pathways (Michallet et al., 2008). After the activation of TLR4 (LPS) and TLR7-TLR8 (R-848), monocyte-derived dendritic cells (MDDCs) from P1 produced smaller amounts of IFN-α, IL-12p40 (Fig. 5A), TNF-α, IL-6, and IL-10 (Fig. S5A) than cells from eight control subjects. Similar results were obtained after the activation of TLR4 and TLR7-TLR8 in monocyte-derived macrophages (MDMs), in terms of the production of IFN-λ, IL-12p40 (Fig. 5B), TNF-α, and IL-6 (Fig S5B). TRAF3 is also involved in the RIG-I and MDA-5 pathway. We therefore tested this pathway in SV40-fibroblasts. After activation with poly(I:C) plus Lipofectamine or *in vitro* transcribed

5’PPP-ssRNA (7sk-as), the amounts of secreted IFN-β, IFN-λ and IL-6 were lower than those of control cells, UNC-93B-deficient cells (Fig. 5C) and P1 SV40-fibroblasts transfected with WT *TRAF3* (Fig. S5C). Poly(I:C) plus Lipofectamine is known to activate both the RIG-I and MDA-5 pathways, whereas *in vitro* transcribed 5’PPP-ssRNA (7sk-as) has been shown to be a RIG-I-specific agonist (Pichlmair et al., 2006). These pathways — the RIG-I pathway in particular — are therefore apparently TRAF3-dependent in human dermal fibroblasts. Finally, we assessed the overall impact of TRAF3 deficiency on the production of type I IFN and IFN-λ, by investigating the response to several viruses in various cell types. After 40 hours of stimulation, peripheral blood mononuclear cells (PBMC) from P1 produced IFN-α (Fig. 5D) and IL-6, IL-10 and IL-12p40 (Fig. S5D, E and F) in response to the 10 viruses tested, in amounts similar to or smaller than those produced by control cells. We investigated the production of IFN-β and IFN-λ in SV40-fibroblasts, after stimulation with HSV-1 (Fig. 5E) and with four other viruses (VSV, para-III, Sindbis virus and EMCV) (Fig. 5F). P1 fibroblasts had a broader phenotype than cells from healthy controls, UNC-93B-deficient, TLR3-deficient and MyD88-deficient patients. Thus, TRAF3 deficiency in the patient broadly affected type I and type III IFN inducing pathways.

Impact of TRAF3 deficiency on TNFR pathways

TRAF3 was initially shown to interact with various TNFRs, such as CD40, LT-βR, and BAFFR, in particular (Bishop and Xie, 2007; He et al., 2007). It was subsequently found to operate downstream from these receptors, as a negative regulator of the alternative NF-κB pathway (He et al., 2006; Vallabhapurapu et al., 2008; Zarnegar et al., 2008). We first analyzed the CD40 pathway (Cheng et al., 1995; Graham et al., 2009). P1 MDDC showed impaired production of IL-6 and IL-12p40

after CD40L activation (Fig. 6A and B). We also activated fresh B cells from P1 (who has normal counts of the main circulating B-cell subsets, as defined by IgM and CD27 expression) with CD40L and IL-4 and observed an impairment of proliferation and Ig class switch recombination to IgE (data not shown). When EBV-B cells from P1 were activated with CD40L, the p52 product was generated without stimulation and was therefore constitutively activated, whereas p52 activation was not constitutive in healthy controls (Fig. S6A). CD40-deficient cells served as negative controls (Conley et al., 2009). TRAF3 is also involved in the lymphotoxin-β receptor (LTβR) pathway in humans and mice, inducing caspase-3-independent cell death and IL-8 production (Chen et al., 2003; Kuai et al., 2003). P1 SV40-fibroblasts displayed lower amounts of cell death than control cells (Fig. 6C) or P1 cells transfected with WT-TRAF3 (Fig. S6B) after LT-α1β2 stimulation. Moreover, P1 cells produced smaller amounts of IL-8 than control cells and P1 SV40-fibroblasts transfected with WT-TRAF3 (P1-WT) (Fig. 6D).

TRAF3 also controls IL-10 production in response to B cell-activating factor receptor (BAFF-R) activation in human and mouse cell lines (Gardam et al., 2008; Sasaki et al., 2008; Xu and Shu, 2002). After the activation of BAFF in EBV-B cells, the p52 product was generated without stimulation (i.e. it was constitutively activated) in cells from P1, but not in cells from healthy controls (Fig. 6E). Similarly, ELISA after BAFF activation in EBV-B cells showed that P1 cells produced more IL-10 than control cells and that this IL-10 production was not dependent on BAFF activation (Fig. 6F). BAFF-R-deficient EBV-B cells were used as negative controls (Warnatz et al., 2009). We conclude that TRAF3 deficiency in P1 affects at least the CD40, LTβR and BAFF-R pathways, as previously shown in mouse and human cell lines. The lack of a corresponding overt clinical phenotype is consistent with an incomplete functional

defect. By contrast, complete defects in CD40 (Conley et al., 2009) and, to a lesser extent, BAFF-R (Warnatz et al., 2009), have been shown to have clinical consequences. We would expect the residual signaling threshold below which predisposition to disease occurs to vary between pathways.

DISCUSSION

We have identified a patient with a heterozygous *de novo* R118W germline mutation in *TRAF3*. Previous studies have identified the R118W mutation of *TRAF3* as a somatic mutation involved in multiple myeloma (Annunziata et al., 2007; Keats et al., 2007), independently indicating that this allele is deleterious and suggesting that our patient might be at risk of this disease. Heterozygosity for the R118W *TRAF3* allele leads to impairment of the TLR3-dependent induction of type I IFN and IFN-λ, resulting in predisposition to HSE. Autosomal dominant TRAF3 deficiency is the third genetic etiology of HSE to be identified, after autosomal recessive UNC-93B deficiency (Casrouge et al., 2006) and autosomal dominant TLR3 deficiency (Zhang et al., 2007). It is a rare genetic etiology of HSE, as no TRAF3 coding mutations have been identified in 190 other children with HSE analyzed. TRAF3 deficiency is also the first primary immunodeficiency involving a TRAF protein to be identified. The presence of TRAF3 deficiency in a child with HSE confirms the importance of an intact TLR3-IFN pathway for controlling primary HSV-1 infection in the CNS (Zhang et al., 2007). It further indicates that TLR3-mediated immunity is not protective with only 10-20% expression and function of TRAF3. Mutations in the *UNC93B*, *TLR3*, *TRIF*, and *TRAF3* genes each affect only a small proportion of children with HSE. These findings suggest that predisposition to HSE may result from a collection of diverse, and possibly immunologically related single-gene defects (Alcais et al., 2009; Casanova and Abel, 2007).

The patient with TRAF3 deficiency and HSE described here is now 18 years old and has otherwise remained healthy off any prophylaxis, with normal resistance to other infectious diseases, including viral diseases in particular. Residual signaling downstream from TLR3 is probably not involved in this resistance, because UNC-93B-

deficient patients have no detectable residual TLR3 signaling but are nonetheless also resistant to common viruses other than HSV-1. Anti-viral IFN responses triggered by receptors other than TLR3, whether TRAF3-dependent (somewhat preserved due to the incomplete nature of TRAF3 deficiency) or TRAF-3-independent (unaffected by the TRAF3 defect), probably account for the normal resistance to viruses observed in this TRAF3-deficient patient. With a single 18-year-old patient studied, it is obviously impossible to draw firm conclusions regarding the range of infectious phenotypes associated with dominant-negative TRAF3 alleles. Other infections may strike this patient later in life, and other patients carrying dominant-negative TRAF3 alleles may display other infectious phenotypes. Phenotypes other than infectious may also occur. The TRAF3 defect also impairs signaling pathways downstream from multiple TNF receptors. However, this broad immunological phenotype has had so far no overt clinical consequences. This may be transient, as for example the impairment of BAFF signaling might perhaps lead to disorders of B cell immunity with increasing age (Warnatz et al., 2009). In any case, the weak but detectable residual TRAF3-dependent responses in this patient probably account for her survival into adulthood, contrasting with the neonatal death of mice with complete TRAF3 deficiency (He et al., 2006; Xu et al., 1996). In conclusion, this “experiment of nature” suggests that the first apparent clinical consequence of decreases in TRAF3 production and function is predisposition to HSE, due to the impairment of TLR3 responses.

EXPERIMENTAL PROCEDURES

Human molecular genetics

We extracted RNA from Epstein-Barr virus-immortalized lymphoblastoid cell lines (EBV-B cells) and immortalized fibroblast cell lines (SV40-fibroblasts), using Trizol (Invitrogen, Carlsbad , California, USA), according to the manufacturer's instructions. RNA was reverse transcribed directly, with Oligo-dT (Invitrogen). Polymerase chain reaction (PCR) was carried out with *Taq* polymerase (Invitrogen), using the GeneAmp PCR System 9700 (Applied Biosystems, Foster City, California, USA). The cDNA exons of *TRAF3* were amplified by PCR. The primer sequences used for the genomic coding region of *TRAF3* are shown below.

The PCR products were purified by ultracentrifugation through Sephadex G-50 Superfine resin (Amersham-Pharmacia-Biotech, Buckinghamshire, UK) and sequenced with the BigDye Terminator Cycle Sequencing Kit (Applied Biosystems). Sequencing products were purified by centrifugation through Sephadex G-50 Superfine resin and sequences were analyzed with an ABI Prism 3700 apparatus (Applied Biosystems).

The mutation was confirmed by the analysis of genomic DNA extracted from erythrocytes/granulocytes, EBV-B cells and SV40-fibroblasts. DNA was isolated by phenol-chloroform extraction, as previously described (Giraffa et al., 2000).

TRAF3 sequencing primers:

Forward primer
1F: ggaccgcgagatgaggaa
2F: gctcctggctccctactctt
3F: taatgctgggacatctgctg
4F: caactcgctcgaaaagaagg
5F: agccagcctttctacactgg
6F: agtagctggggaggtggatt

Reverse primer
1R: cggtcagtgtgcagctttag
2R: ctcgcaggtctttcctcaag
3R: gcttggctgtctatcactcg

4R: cgtccccgttcaggtagac
5R: aaaacgtgtcaggtgtgctc
6R: actgtatttgaaacaaaattgcac

Multiple amino-acid sequence alignment

The *Homo sapiens* TRAF3 (NP_003291.2) amino-acid sequence was aligned with other TRAF3 sequences by BLAST, using the protein database of the National Center for Biotechnology Information website (NCBI, http://blast.ncbi.nlm.nih.gov/Blast.cgi). Multiple sequence alignment was carried out with CLUSTAL W (1.83), based on the TRAF3 amino-acid sequences of *Pan troglodytes* (XP_001164813), *Macaca mulatta* (XP_001082535.1), *Equus caballus* (XP_001490050.1), *Monodelphis domestica* (XP_001367040.1), *Ornithorhynchus anatinus* (XP_001507440.1), *Mus musculus* (NP_035762.2), *Sus scrofa* (XP_001927435.1), *Rattus norvegicus* (NP_001102194.1), *Bos taurus* (XP_582595.3), *Canis familiaris* (XP_547989.2), *Gallus gallus* (XP_421378.1), *Oncorhynchus mykiss* (XP_001507398.1) and *Danio rerio* (NP_001003513.1).

Cell purification and culture

Freshly isolated human peripheral blood mononuclear cells (PBMC) were isolated by Ficoll-Hypaque density gradient centrifugation (Amersham-Pharmacia-Biotech) from cytopheresis or whole-blood samples obtained from patients or healthy volunteers. PBMCs were stimulated for 40 h, at a density of 2 x 10^6 cells/ml, in RPMI 1640 (Invitrogen) supplemented with 10% fetal calf serum (FCS) (Invitrogen).

Primary human fibroblasts were obtained from biopsies of patients or healthy controls, and were cultured in DMEM (Invitrogen) supplemented with 10% FCS. They were then transformed with an SV40 vector, as previously described (Chapgier et al., 2006), to create immortalized fibroblast cell lines: SV40-fibroblasts. The SV40-

fibroblast cell lines were activated in 24-well plates, at a density of 10^5 cells/well, for 24 h (or 2, 10 and 24 h in the poly(I:C) kinetic studies).

EBV-B cell lines were obtained from patients and normal donors as previously described (Pellat-Deceunynck et al., 1999). $BAFFR^{-/-}$ EBV-B cells were kindly provided by Klaus Warnatz, PhD. EBV-B cells were cultured in RPMI medium supplemented with 10% FCS and were activated in 6-well plates, at a density of 5 $x10^6$ cells/well, for 24 h.

For the differentiation and culture of monocyte-derived dendritic cells (MDDCs), PBMCs freshly isolated by Ficoll-Hypaque density gradient centrifugation from healthy controls and patients, were incubated in RPMI 1640 supplemented with 10% FCS, in cell culture flasks, for 1 hour, at 37°C, under an atmosphere containing 5% CO_2. The adherent cells (monocytes) were cultured for 8 days in RPMI 1640 supplemented with 10% FCS, in the presence of GM-CSF (R&D Systems, Minneapolis, MN, USA, 50 ng/ml) and IL-4 (R&D Systems, 10 ng/ml). The differentiation and purity of these cells were confirmed by staining with antibodies directed against CD1a (PE, BD Pharmingen, San Diego, CA, USA) and CD14 (FITC, Becton Dickinson) or a conjugated mouse IgG1 isotype control (PE or FITC, Becton Dickinson). Stained cells were analyzed by flow cytometry (FACSCanto flow cytometer, Becton Dickinson). For stimulation, the cells were plated at a density of 0.25 x 10^5 cells/well in 48-well tissue culture plates and cultured in the presence of GM-CSF and IL-4; MDDCs were stimulated for 24 h.

For the differentiation and culture of monocyte-derived macrophages (MDM), PBMCs freshly isolated by Ficoll-Hypaque density gradient centrifugation from healthy controls and patients were incubated in RPMI 1640 supplemented with 10% FCS, in cell culture flasks, for 1 hour, at 37°C, under an atmosphere containing 5% CO_2. The

adherent cells (monocytes) were cultured for 10 days in RPMI 1640 supplemented with 10% FCS, in the presence of Rh-M-CSF (R&D Systems, 10 µg/ml). For stimulation, the cells were plated at a density of 0.25 x 10^5 cells/well in 96-well tissue culture plates and stimulated for 24 h.

All cells were grown at 37°C, under an atmosphere containing 5% CO_2.

Determination of mRNA levels by Q-PCR

Total RNA was extracted from EBV-B cells, SV40-fibroblasts RAW, and RAWTRAF3$^{-/-}$ cells, untransfected or transfected. In some cases, the cells were stimulated with 25 µg/ml poly(I:C) (InvivoGen, San Diego, CA, USA) for 4 hours. RNA was reverse transcribed directly, using Oligo-dT, to determine TRAF3, IFN-β and IFN-λ mRNA levels. The β-glucuronidase (GUS) or 18S rRNA gene was used for normalization. Quantitative real-time PCR (Q-PCR) was performed with Applied Biosystems Assays-on-Demand™ probe/primer combinations and 2 x universal reaction mixture, in an ABI PRISM® 7700 Sequence Detection System. Results are expressed using the ΔΔCt method, as described by the manufacturer.

Immunoblots

Total cell extracts were prepared from SV40-fibroblasts, EBV-B cells and RAW and RAW-TRAF3$^{-/-}$ cells, either not transfected or stably transfected with pWPI, pWPI-TRAF3, pBABE or pBABE-TRAF3-R118W. In some cases, SV40-fibroblasts were activated by incubation with 25 µg/ml poly(I:C) for 24 h. Equal amounts of protein from each sample were separated by SDS-PAGE and blotted onto iBlot ^{TM} Gel Transfer Stacks (Invitrogen). These nitrocellulose membranes were then probed with anti-TRAF3 polyclonal antibody (Abcam, Cambridge, MA, USA) or anti-NF-kB2 p100/p52

(18D10) rabbit mAb (human specific) (Cell Signaling Beverly, MA, USA) followed by a secondary horseradish-conjugated donkey anti-rabbit IgG (GE Healthcare**,** Buckinghamshire**,** UK). Membranes were stripped and reprobed with an antibody against GADPH (Santa Cruz Biotechnology Inc., Santa Cruz, CA), to control for protein loading. Antibody binding was detected by enhanced chemiluminescence (ECL; Amersham-Pharmacia-Biotech). Antibody-2 is an anti-TRAF3 polyclonal antibody (Cell Signaling Technology).

Stimulations

We used the following Toll-like receptor (TLR) agonists: a synthetic analog of dsRNA, polyinosinepolycytidylic acid (poly(I:C), a TLR-3 agonist, at a concentration of 25 µg/ml); lipopolysaccharide (LPS Re 595 from *Salmonella minnesota*, a TLR-4 agonist, at 10 µg/ml; Sigma, St Louis, MO, USA); resiquimod hydrochloride (R-848, a TLR-7 and -8 agonist, at 3 µg/ml; GLSynthesis Inc., Worcester, MA, USA); IL-1β (at 20 ng/ml; R&D Systems Inc.); TNF-α (at 20 ng/ml; R&D Systems Inc.). All agonists and reagents were endotoxin-free. For all stimulations of PBMCs with TLR agonists other than LPS, cells were incubated with polymyxin B (10 µg/ml) (Sigma) at 37°C, for 30 minutes before activation.

For RIG-I/MDA5 stimulation, we used 0.25 µg of poly(I:C) or 0.1 µg of non coding RNA (7sk-as), kindly provided by Caetano Reis e Sousa (Pichlmair et al., 2006), and carried out transfection with Lipofectamine^{TM} Reagent (Invitrogen), according to the kit manufacturer's instructions.

LTα1β2 (R&D Systems, 65 ng/ml) was used to activate lymphotoxin-β receptor (LTβR), with or without IFN-γ (Imukin; Boehringer Ingelheim, Ingelheim, Germany), at a concentration of 80 IU/ml. B cell-activating factor receptor (BAFF-R) was activated

with human BAFF (Miltenyi Biotec, Bergisch Gladbach, Germany) at a concentration of 100 ng/ml.

For viral stimulation, we used: 1) dsDNA viruses: herpes simplex virus-1 (HSV-1, strain KOS-1, multiplicity of infection (MOI) = 1); HSV-1 inactivated by ultraviolet (UV) radiation (HSV-1i); BK virus (BKV, an isolate from a patient, provided by Pierre Lebon, Paris, France, MOI= 0.02). 2) ss(-)RNA viruses: vesicular stomatitis virus (VSV, strain Indiana, MOI= 1), Newcastle disease virus (NDV, strain BR24 444, MOI = 0.5), measles virus (measles V, strain Edmonston, MOI = 0.004), Sendai virus (Sendai V, strain E92, MOI= 12.5), parainfluenza virus III (para-III, strain EA102, MOI= 0.04), mumps virus (mumps V, vaccine strain Urabe, MOI = 0.04). 3) ss(+)RNA viruses: sindbis virus (sindbis V, strain VR1248 ATCC, MOI= 0.2), encephalomyocarditis virus (EMCV, MOI = 0.1).

In some experiments, cells were treated with IFN-α (intron A, Schering-Plough, Kenilworth, NJ, USA) at a concentration of 10^5 IU/ml before stimulation. CD40 was activated in MDDC, as previously described (Filipe-Santos et al., 2006). In EBV-B cells, CD40 was activated with soluble human MegaCD40L^{TM}(ENZO Life Science Inc., Farmingdale, NY, USA) at a concentration of 2 µg/ml.

Cell supernatants were recovered and their cytokine concentrations determined by ELISA.

Cytokine determinations

The production of IFN-α, -β, -λ, IL-6, IL-8, IL-10, IL-12p40 and TNF-α was assessed by ELISA. An ELISA was carried out for each of IFN-α (AbCys SA, Paris, France), IFN-β (TFB, Fujirebio, Inc., Tokyo, Japan), IL-6, IL-8, IL-10, TNF-α (Sanquin, Amsterdam, Holland), IL-12p40 and mouse IFN-β (R&D Systems),

according to the kit manufacturer's instructions. The ELISA for IFN-λ was carried out as previously described (Zhang et al., 2007).

Signal transduction studies in SV40-fibroblasts

Cell nuclear extracts were prepared from SV40-fibroblasts, following incubation with or without Poly(I:C), TNF-α and IL-lβ. NFkB ELISA (Active Motif, Calrsbad, CA, USA) was carried out according to the kit manufacturer's instructions.

For the detection of IRF-3 dimerization, whole-cell extracts were prepared from SV40-fibroblasts with or without Poly(I:C) (25 µg/ml) treatment for 1 or 2 h. The IRF-3 monomers and dimers were separated by native PAGE in the presence of 1% sodium deoxycholate (DOC) (Sigma). Total cell extracts (50 µg of protein) were diluted 1:5 in non denaturing sample buffer (312.5 mM Tris–HCl, pH 6.8, 50% glycerol, 0.05% bromophenol blue and 5% DOC) and separated by electrophoresis in a 7.5% polyacrylamide gel, in 25 mM Tris and 192 mM glycine, pH 8.4, with 1% DOC present in the cathode chamber only. The gel was blotted onto a membrane, which was then probed with the anti-IRF-3 antibody (FL-425, Santa Cruz Biotechnology) followed by a secondary horseradish-conjugated anti-rabbit IgG.

Cell viability assay

The viability of SV40-fibroblasts was assessed by resazurin oxidoreduction (TOX-8) (Sigma). Cells were plated, in triplicate, in 96-well flat-bottomed plates (2 x 10^4 cells/well), in DMEM supplemented with 2% FCS; 24 hours later, cells were infected by incubation for 24 hours with VSV at the indicated multiplicity of infection (MOI). Resazurin dye solution was then added (5 µl per well) to the culture medium, and the samples were incubated for an additional two hours at 37°C. Fluorescence was

then measured at a wavelength of 590 nm, using an excitation wavelength of 531 nm. Background fluorescence, calculated for dye and complete medium alone (in the absence of cells) was then subtracted from the values for all the other samples; 100% viability corresponds to the fluorescence of uninfected cells. For assays of cell protection upon viral stimulation, cells were treated with IFN-α (10^5 IU/ml) for 24 hours before infection, and during infection.

Viral infection

For viral infection, 10^5 SV40-fibroblasts were plated in individual wells of 24-well plates and infected, at a MOI of 10, in DMEM supplemented with 2% FCS. The Stat-1-deficient patient studied has been described elsewhere (*2*). After 30 minutes, cells were washed and incubated in 500 µl of medium. The supernatants were frozen at the time points indicated in the figures. Viral titers were determined by calculating the 50% tissue culture infectious dose ($TCID_{50}$), as described by Reed and Muench, after the inoculation of Vero cell cultures in 96-well plates. For assays of cell protection upon viral stimulation, cells were treated with IFN-α (10^5 IU/ml) for 18 hours before infection, as appropriate.

Determination of cell death via the LTβR pathway

We assessed levels of SV40-fibroblast cell death via the LTβR pathway by TOX-8 assays. Cells were plated, in triplicate, in 96-well flat-bottomed plates (2×10^4 cells/well), in DMEM supplemented with 2% FCS; 24 hours later, cells were treated with LTα1β2 (65 or 100 ng/ml), with or without IFN-γ at a concentration of 80 IU/ml and incubated for 72 h. Resazurin dye solution was then added (5 µl per well) to the culture medium, and the samples were incubated for an additional two hours at 37°C.

Fluorescence was then measured at a wavelength of 590 nm, using an excitation wavelength of 531 nm. Background fluorescence, calculated for dye and complete medium alone (in the absence of cells) was then subtracted from the values for all the other samples; 100% viability corresponds to the fluorescence of non stimulated cells.

Site-directed mutagenesis and cloning

Site-directed mutagenesis was performed with QuikChange®II XL (Stratagene, La Jolla, CA, USA), using the pCR4.0-TRAF3 plasmid (kindly provided by Jonathan Keats, PhD). The TRAF3-R118W gene generated by mutagenesis was inserted into the pBABE-puro expression vector (Addgene, Cambridge, MA, USA) (pBABE-TRAF3-R118W).

Two TRAF3 C-terminal deletions without amino acids 289-568 were created in the pBABE-puro expression vector:

- pBABE-TRAF3-Δ(289-568)
- pBABE-TRAF3-R118W-Δ(289-568)

Stable transfections

Cells (SV40-fibroblasts, RAW and RAW-TRAF3$^{-/-}$ cells (kindly provided by Michael Karin, PhD)) were transfected by electroporation at 250 V and 960 mF, in phosphate-buffered saline (10^7 cells/ 0.5 ml). We used 5 µg of pWPI-TRAF3 (kindly provided by Jonathan Keats, PhD) or pBABE-TRAF3-R118W, linearized with *Fsp*I (New England Biolabs, Beverly, MA, USA), for transfection. Transfectants were selected by sorting cells expressing green fluorescent protein (GFP) for pWPI-TRAF3, or in 0.5 mg/ml puromycin 24 h after electroporation for pBABE-TRAF3-R118W. The

presence of TRAF3 was checked by Q-PCR and western blotting. The same conditions were used for the transfection of cells with mock vectors.

Transient transfections

RAW and RAW-TRAF3$^{-/-}$ cells were transfected with 2 µg of plasmid (all derived from the pBABE-puro expression vector) at various ratios, in the presence of the FuGENE ®HD Transfection Reagent (Roche Applied Science, Indianapolis, IN, USA), according to the kit manufacturer's instructions.

ACKNOWLEDGMENTS

We thank the members of the Laboratory of Human Genetics of Infectious Diseases, and J. Keats, R. Miller, L. Zitvogel, S. Matikainen, C. Reis e Sousa, S. Plebani and D. W. Leaman for reagents. We thank the patient and her family for their participation in this study, which was supported by the AXA Research fund, the Schlumberger Foundation, the BNP-Paribas Foundation, the *Groupement d'Intérêt Scientifique Maladies Rares*, the *Action Concertée Incitative de Microbiologie*, the March of Dimes, the *Agence Nationale pour la Recherche*, the Eppley Foundation, the National Institute of Allergy and Infectious Diseases grant number 1R01AI088364, the Thrasher Research Fund, the Jeffrey Modell Foundation and Talecris Biotherapeutics, the St. Giles Foundation, the Rockefeller University Center for Clinical and Translational Science grant number 5UL1RR024143, and the Rockefeller University. P.R. is supported by a European Union FP6 grant. J.-L.C. was an international scholar of the Howard Hughes Medical Institute until 2008.

REFERENCES

Abel, L., Plancoulaine, S., Jouanguy, E., Zhang, S.Y., Mahfoufi, N., Nicolas, N., Sancho-Shimizu, V., Alcais, A., Guo, Y., Cardon, A., *et al.* Age-dependent Mendelian predisposition to herpes simplex virus type 1 encephalitis in childhood. J Pediatr.

Alcais, A., Abel, L., and Casanova, J.L. (2009). Human genetics of infectious diseases: between proof of principle and paradigm. J Clin Invest *119*, 2506-2514.

Annunziata, C.M., Davis, R.E., Demchenko, Y., Bellamy, W., Gabrea, A., Zhan, F., Lenz, G., Hanamura, I., Wright, G., Xiao, W., *et al.* (2007). Frequent engagement of the classical and alternative NF-kappaB pathways by diverse genetic abnormalities in multiple myeloma. Cancer Cell *12*, 115-130.

Bishop, G.A., and Xie, P. (2007). Multiple roles of TRAF3 signaling in lymphocyte function. Immunol Res *39*, 22-32.

Casanova, J.L., and Abel, L. (2007). Primary immunodeficiencies: a field in its infancy. Science *317*, 617-619.

Casrouge, A., Zhang, S.Y., Eidenschenk, C., Jouanguy, E., Puel, A., Yang, K., Alcais, A., Picard, C., Mahfoufi, N., Nicolas, N., *et al.* (2006). Herpes simplex virus encephalitis in human UNC-93B deficiency. Science *314*, 308-312.

Conley, M.E., Dobbs, A.K., Farmer, D.M., Kilic, S., Paris, K., Grigoriadou, S., Coustan-Smith, E., Howard, V., and Campana, D. (2009). Primary B cell immunodeficiencies: comparisons and contrasts. Annu Rev Immunol *27*, 199-227.

Chapgier, A., Kong, X.F., Boisson-Dupuis, S., Jouanguy, E., Averbuch, D., Feinberg, J., Zhang, S.Y., Bustamante, J., Vogt, G., Lejeune, J., *et al.* (2009). A partial form of recessive STAT1 deficiency in humans. J Clin Invest *119*, 1502-1514.

Chapgier, A., Wynn, R.F., Jouanguy, E., Filipe-Santos, O., Zhang, S., Feinberg, J., Hawkins, K., Casanova, J.L., and Arkwright, P.D. (2006). Human complete Stat-1 deficiency is associated with defective type I and II IFN responses *in vitro* but immunity to some low virulence viruses *in vivo*. J Immunol *176*, 5078-5083.

Chen, M.C., Hwang, M.J., Chou, Y.C., Chen, W.H., Cheng, G., Nakano, H., Luh, T.Y., Mai, S.C., and Hsieh, S.L. (2003). The role of apoptosis signal-regulating kinase 1 in lymphotoxin-beta receptor-mediated cell death. J Biol Chem *278*, 16073-16081.

Cheng, G., Cleary, A.M., Ye, Z.S., Hong, D.I., Lederman, S., and Baltimore, D. (1995). Involvement of CRAF1, a relative of TRAF, in CD40 signaling. Science *267*, 1494-1498.

De Tiege, X., Rozenberg, F., and Heron, B. (2008). The spectrum of herpes simplex encephalitis in children. Eur J Paediatr Neurol *12*, 72-81.

Dupuis, S., Jouanguy, E., Al-Hajjar, S., Fieschi, C., Al-Mohsen, I.Z., Al-Jumaah, S., Yang, K., Chapgier, A., Eidenschenk, C., Eid, P., *et al.* (2003). Impaired response to interferon-alpha/beta and lethal viral disease in human STAT1 deficiency. Nat Genet *33*, 388-391.

Filipe-Santos, O., Bustamante, J., Haverkamp, M.H., Vinolo, E., Ku, C.L., Puel, A., Frucht, D.M., Christel, K., von Bernuth, H., Jouanguy, E., *et al.* (2006). X-linked susceptibility to mycobacteria is caused by mutations in NEMO impairing CD40-dependent IL-12 production. J Exp Med *203*, 1745-1759.

Gardam, S., Sierro, F., Basten, A., Mackay, F., and Brink, R. (2008). TRAF2 and TRAF3 signal adapters act cooperatively to control the maturation and survival signals delivered to B cells by the BAFF receptor. Immunity *28*, 391-401.

Giraffa, G., Rossetti, L., and Neviani, E. (2000). An evaluation of chelex-based DNA purification protocols for the typing of lactic acid bacteria. J Microbiol Methods *42*, 175-184.

Graham, J.P., Moore, C.R., and Bishop, G.A. (2009). Roles of the TRAF2/3 binding site in differential B cell signaling by CD40 and its viral oncogenic mimic, LMP1. J Immunol *183*, 2966-2973.

Hacker, H., Redecke, V., Blagoev, B., Kratchmarova, I., Hsu, L.C., Wang, G.G., Kamps, M.P., Raz, E., Wagner, H., Hacker, G., *et al.* (2006). Specificity in Toll-like receptor signalling through distinct effector functions of TRAF3 and TRAF6. Nature *439*, 204-207.

He, J.Q., Oganesyan, G., Saha, S.K., Zarnegar, B., and Cheng, G. (2007). TRAF3 and its biological function. Adv Exp Med Biol *597*, 48-59.

He, J.Q., Zarnegar, B., Oganesyan, G., Saha, S.K., Yamazaki, S., Doyle, S.E., Dempsey, P.W., and Cheng, G. (2006). Rescue of TRAF3-null mice by p100 NF-kappa B deficiency. J Exp Med *203*, 2413-2418.

Hoebe, K., and Beutler, B. (2006). TRAF3: a new component of the TLR-signaling apparatus. Trends Mol Med *12*, 187-189.

Keats, J.J., Fonseca, R., Chesi, M., Schop, R., Baker, A., Chng, W.J., Van Wier, S., Tiedemann, R., Shi, C.X., Sebag, M., *et al.* (2007). Promiscuous mutations activate the noncanonical NF-kappaB pathway in multiple myeloma. Cancer Cell *12*, 131-144.

Kuai, J., Nickbarg, E., Wooters, J., Qiu, Y., Wang, J., and Lin, L.L. (2003). Endogenous association of TRAF2, TRAF3, cIAP1, and Smac with lymphotoxin beta receptor reveals a novel mechanism of apoptosis. J Biol Chem *278*, 14363-14369.

Michallet, M.C., Meylan, E., Ermolaeva, M.A., Vazquez, J., Rebsamen, M., Curran, J., Poeck, H., Bscheider, M., Hartmann, G., Konig, M., *et al.* (2008). TRADD protein is an essential component of the RIG-like helicase antiviral pathway. Immunity *28*, 651-661.

Oganesyan, G., Saha, S.K., Guo, B., He, J.Q., Shahangian, A., Zarnegar, B., Perry, A., and Cheng, G. (2006). Critical role of TRAF3 in the Toll-like receptor-dependent and -independent antiviral response. Nature *439*, 208-211.

Pellat-Deceunynck, C., Jego, G., Harousseau, J.L., Vie, H., and Bataille, R. (1999). Isolation of human lymphocyte antigens class I-restricted cytotoxic T lymphocytes against autologous myeloma cells. Clin Cancer Res *5*, 705-709.

Picard, C., Puel, A., Bonnet, M., Ku, C.L., Bustamante, J., Yang, K., Soudais, C., Dupuis, S., Feinberg, J., Fieschi, C., *et al.* (2003). Pyogenic bacterial infections in humans with IRAK-4 deficiency. Science *299*, 2076-2079.

Pichlmair, A., Schulz, O., Tan, C.P., Naslund, T.I., Liljestrom, P., Weber, F., and Reis e Sousa, C. (2006). RIG-I-mediated antiviral responses to single-stranded RNA bearing 5'-phosphates. Science *314*, 997-1001.

Pullen, S.S., Labadia, M.E., Ingraham, R.H., McWhirter, S.M., Everdeen, D.S., Alber, T., Crute, J.J., and Kehry, M.R. (1999). High-affinity interactions of tumor necrosis factor receptor-associated factors (TRAFs) and CD40 require TRAF trimerization and CD40 multimerization. Biochemistry *38*, 10168-10177.

Sasaki, Y., Calado, D.P., Derudder, E., Zhang, B., Shimizu, Y., Mackay, F., Nishikawa, S., Rajewsky, K., and Schmidt-Supprian, M. (2008). NIK overexpression amplifies, whereas ablation of its TRAF3-binding domain replaces BAFF:BAFF-R-mediated survival signals in B cells. Proc Natl Acad Sci USA *105*, 10883-10888.

Tseng, P.H., Matsuzawa, A., Zhang, W., Mino, T., Vignali, D.A., and Karin, M. (2010). Different modes of ubiquitination of the adaptor TRAF3 selectively activate the expression of type I interferons and proinflammatory cytokines. Nat Immunol *11*, 70-75.

Vallabhapurapu, S., Matsuzawa, A., Zhang, W., Tseng, P.H., Keats, J.J., Wang, H., Vignali, D.A., Bergsagel, P.L., and Karin, M. (2008). Nonredundant and complementary functions of TRAF2 and TRAF3 in a ubiquitination cascade that activates NIK-dependent alternative NF-kappaB signaling. Nat Immunol *9*, 1364-1370.

von Bernuth, H., Picard, C., Jin, Z., Pankla, R., Xiao, H., Ku, C.L., Chrabieh, M., Mustapha, I.B., Ghandil, P., Camcioglu, Y., *et al.* (2008). Pyogenic bacterial infections in humans with MyD88 deficiency. Science *321*, 691-696.

Warnatz, K., Salzer, U., Rizzi, M., Fischer, B., Gutenberger, S., Bohm, J., Kienzler, A.K., Pan-Hammarstrom, Q., Hammarstrom, L., Rakhmanov, M., *et al.* (2009). B-cell activating factor receptor deficiency is associated with an adult-onset antibody deficiency syndrome in humans. Proc Natl Acad Sci USA *106*, 13945-13950.

Whitley, R.J. (2006). Herpes simplex encephalitis: adolescents and adults. Antiviral Res *71*, 141-148.

Xu, L.G., and Shu, H.B. (2002). TNFR-associated factor-3 is associated with BAFF-R and negatively regulates BAFF-R-mediated NF-kappa B activation and IL-10 production. J Immunol *169*, 6883-6889.

Xu, Y., Cheng, G., and Baltimore, D. (1996). Targeted disruption of TRAF3 leads to postnatal lethality and defective T-dependent immune responses. Immunity *5*, 407-415.

Yang, K., Puel, A., Zhang, S., Eidenschenk, C., Ku, C.L., Casrouge, A., Picard, C., von Bernuth, H., Senechal, B., Plancoulaine, S., *et al.* (2005). Human TLR-7-, -8-, and -9-mediated induction of IFN-alpha/beta and -lambda Is IRAK-4 dependent and redundant for protective immunity to viruses. Immunity *23*, 465-478.

Zarnegar, B.J., Wang, Y., Mahoney, D.J., Dempsey, P.W., Cheung, H.H., He, J., Shiba, T., Yang, X., Yeh, W.C., Mak, T.W., *et al.* (2008). Noncanonical NF-kappaB activation requires coordinated assembly of a regulatory complex of the adaptors cIAP1, cIAP2, TRAF2 and TRAF3 and the kinase NIK. Nat Immunol *9*, 1371-1378.

Zhang, S.Y., Jouanguy, E., Ugolini, S., Smahi, A., Elain, G., Romero, P., Segal, D., Sancho-Shimizu, V., Lorenzo, L., Puel, A., *et al.* (2007). TLR3 deficiency in patients with herpes simplex encephalitis. Science *317*, 1522-1527.

FIGURE LEGENDS

Fig. 1. Heterozygous *TRAF3* mutation in a child with HSE (P1)

(A) Family pedigree, with allele segregation. The patient with HSE, in black, is heterozygous for the mutation. **(B)** Heterozygous c.352C>T mutation in patient 1 (P1). The sequence of the polymerase chain reaction products of genomic DNA from leukocytes of a control (C) and P1 is shown. (**C**) Schematic representation of TRAF3 protein structure. Human *TRAF3* has eleven exons, encoding a protein composed of a ring finger and five zinc-finger domains in the N-terminal region, followed by an isoleucine zipper and a TRAF domain in the C-terminal region. P1 carries the c.352C>T mutation, which results in an arginine (R) to tryptophan (W) substitution at amino-acid position 118 (R118W) in the first zinc-finger domain.

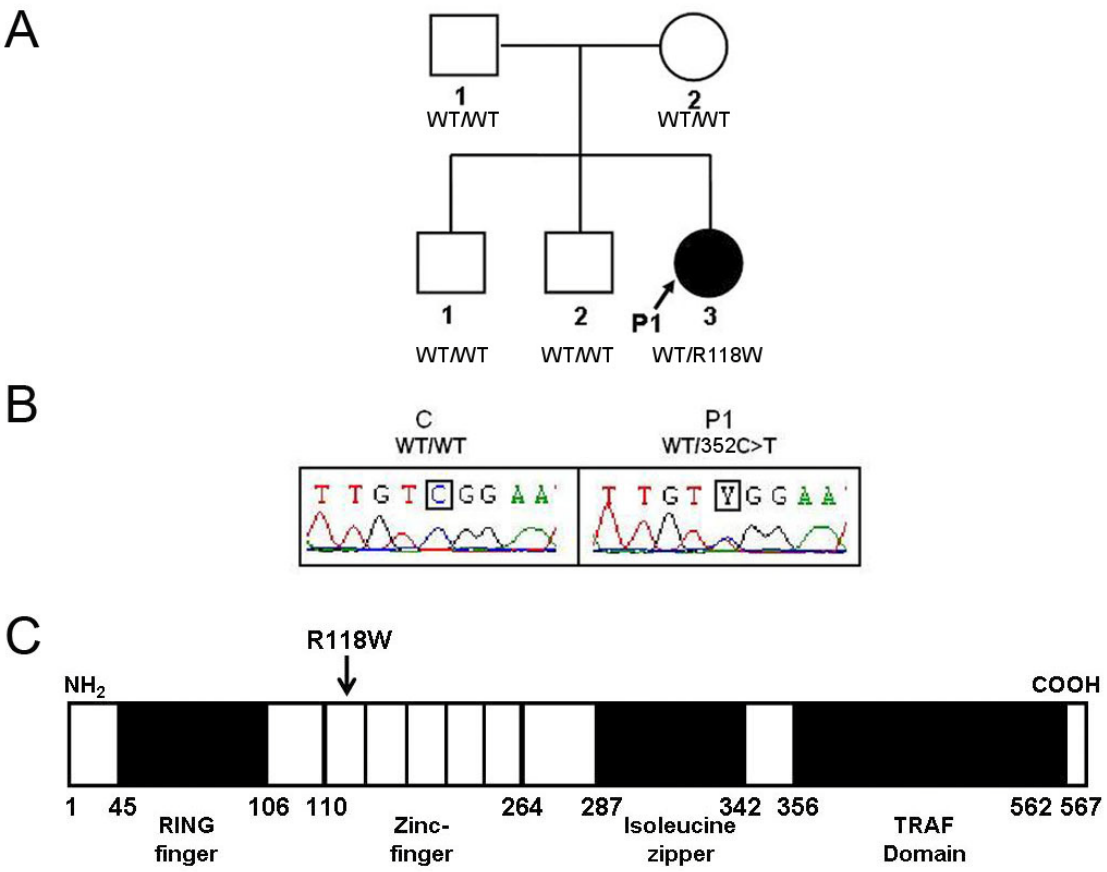

Fig. 2. *TRAF3* expression levels and TLR3 response of a child with HSE (P1)

(**A**) *(Top)* TRAF3 mRNA expression in SV40-fibroblasts from a control (C) and P1. β-glucuronidase (GUS) was used for normalization. *(Bottom)* Representative immunoblot analysis of TRAF3 in SV40-fibroblasts from a control (C) and P1. TRAF3 (%) indicates densitometry results, normalized with respect to GADPH and expressed as a percentage of control TRAF3. The control is a representative example of the five controls analyzed. **(B)** *(Top)* TRAF3 mRNA levels normalized with respect to 18S rRNA and *(Bottom)* immunoblot analysis of TRAF3 in RAW cells and RAW *Traf3*$^{-/-}$ cells not transfected and stably transfected with human wild-type (WT) (pWPI-TRAF3) or R118W mutant *TRAF3* (pBABE-TRAF3-R118W) constructs. As a negative control, we transfected cells with a mock WT vector (Mock-1, pWPI) or with a mock R118W mutant vector (Mock-2, pBABE). TRAF3 (%) indicates densitometry results normalized with respect to GADPH amounts and expressed as a percentage of TRAF3 amounts in RAW cells. **(C)** Production of IFN-β (measured in structural units, IU/ml)**,** IFN-λ and IL-6 by SV40-fibroblasts after poly(I:C) stimulation (25 μg/ml), at various time points (*left panels*) and for various doses of poly(I:C), for 24 hours (*right panels*), as assessed by ELISA. C is the positive control and P1 is patient 1; *UNC93B*$^{-/-}$ is the UNC-93B-deficient patient. **(D)** NF-κB ELISA of nuclear extracts from SV40-fibroblasts from a control (C), P1 and a NEMO-deficient patient (negative control), after stimulation with TNF-α and IL-1β for 30 minutes, or stimulation with poly(I:C) for 120 minutes. **(E)** IRF-3 monomers and dimers in total cell extracts of SV40-fibroblasts from a control (C) and P1, after stimulation with poly(I:C) for 1 and 2 hours, as assessed by immunoblot. TLR3- and UNC-93B-deficient patients were used as negative controls.

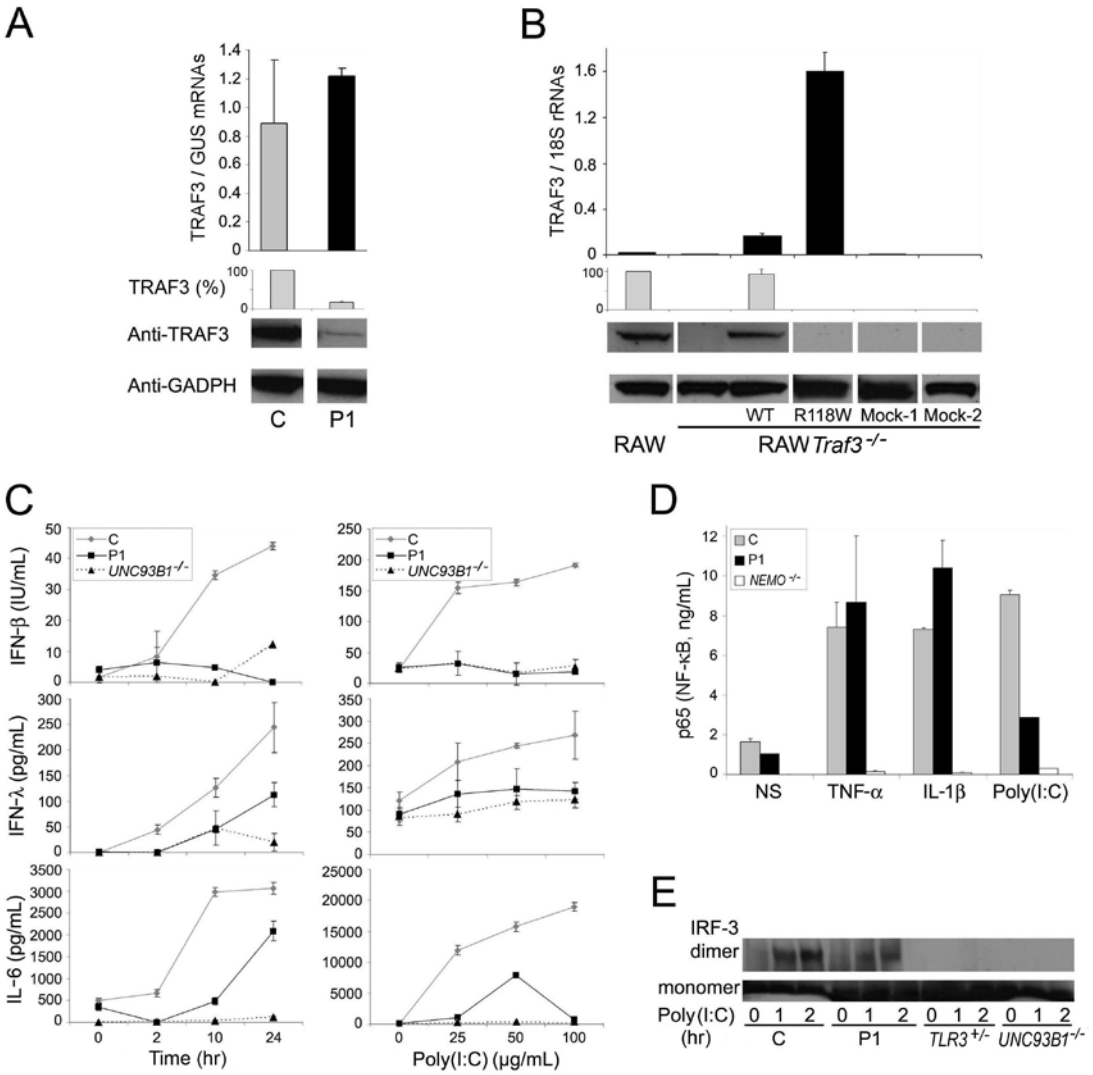
A
TRAF3 / GUS mRNAs
TRAF3 (%)
Anti-TRAF3
Anti-GADPH
C
P1
B
TRAF3 / 18S rRNAs
WT
R118W
Mock-1
Mock-2
RAW
RAW Traf3 -/-
C
IFN-β (IU/mL)
IFN-λ (pg/mL)
IL-6 (pg/mL)
P1
UNC93B1 -/-
Time (hr)
Poly(I:C) (μg/mL)
D
p65 (NF-κB, ng/mL)
NEMO -/-
NS
TNF-α
IL-1β
Poly(I:C)
E
IRF-3
dimer
monomer
Poly(I:C)
(hr)
TLR3 +/-
UNC93B1 -/-

Fig. 3. Complementation of the patient's cells and dominant negative effect

(A) Immunoblot analysis of TRAF3 amounts in SV40-fibroblasts from a control (C) and P1, not transfected (P1) and stably transfected with human WT *TRAF3* (P1 WT) or mock vector (P1-mock), with and without stimulation with poly(I:C) for 24 h. TRAF3 (%) indicates densitometry results normalized with respect to GADPH amounts and expressed as a percentage of control TRAF3 amounts. **(B)** Production of IFN-β and IL-6, as assessed by ELISA, in SV40-fibroblasts from a control (C), P1, an UNC-93B-deficient patient (*UNC93B*$^{-/-}$), P1 cells transfected with human WT *TRAF3* (P1-WT) or mock vector (P1-mock). **(C)** Immunoblot analysis of TRAF3 amounts in RAW cells, non transfected RAW *Traf3*$^{-/-}$ cells, and RAW cells stably transfected with R118W mutant *TRAF3* (R118W), WT *TRAF3* (WT) or mock vector (Mock). **(D)** IFN-β production, as assessed by ELISA, in RAW cells, not transfected or transfected with R118W mutant *TRAF3* or mock vector. All transfections generated stable cell lines. Glyceraldehyde phosphate dehydrogenase (GADPH) was used as an internal expression control for WB. The panels illustrate results from a single experiment, representative of three. Mean values $\pm$ SD were calculated from three independent experiments.

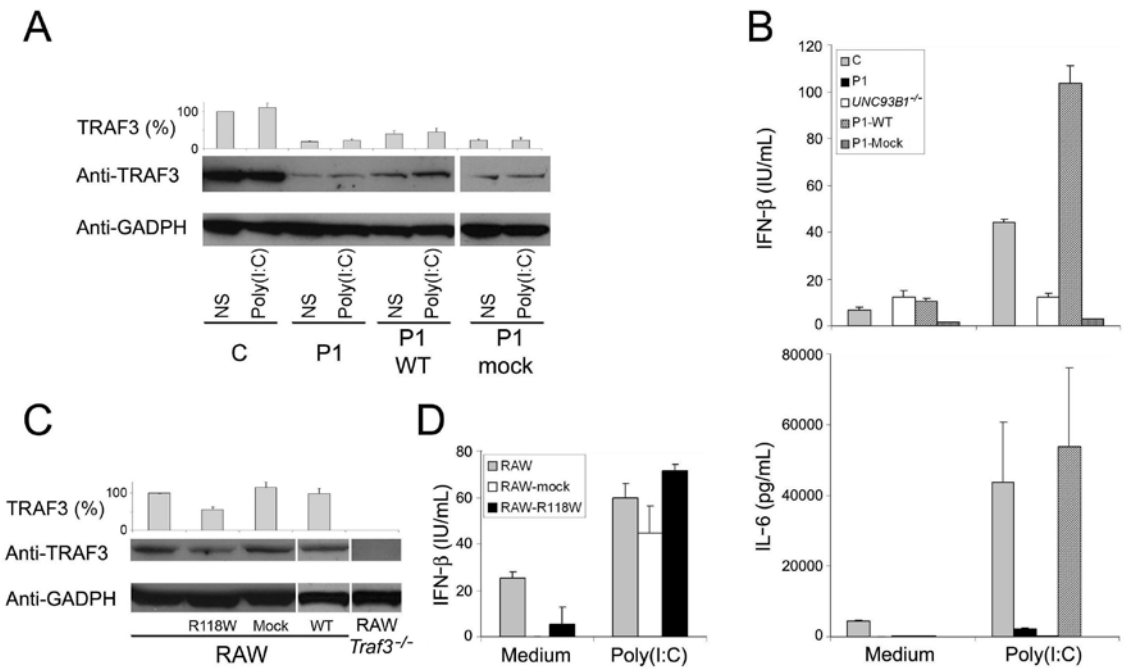

Fig. 4. SV40-fibroblast studies: production of type I IFN and cytokines

(A) Production of IFN-β, IFN-λ and IL-6 after stimulation with VSV, as assessed by ELISA, in SV40-fibroblasts from a control (C), P1 and an UNC-93B-deficient patient (*UNC93B*$^{-/-}$). **(B)** Viable cell percentages, estimated by resazurin oxidation/reduction, for SV40-fibroblasts from a healthy control (C), P1, *TLR3*$^{+/-}$, *UNC93B*$^{-/-}$ and *STAT1*$^{-/-}$ patients, 24 h after infection with VSV, at various multiplicities of infection. The cells were either not treated (left panel), or were subjected to prior treatment (right panel) with recombinant IFN-α for 18 hours. **(C)** VSV titers, estimated on Vero cells, in SV40-fibroblasts from a healthy control (C), P1, *STAT1* $^{-/-}$, *UNC93B* $^{-/-}$ *and TLR3* $^{+/-}$ patients, at various times after VSV infection without (left panel) or with (right panel) 18 hours of pretreatment with IFN-α. **(D)** The production of IFN-β and IL-6, assessed by ELISA, in SV40-fibroblasts from a control (C), P1 (*UNC93B* $^{-/-}$), P1 SV40-fibroblasts transfected with human WT *TRAF3* (P1-WT) or mock vector (P1-mock). **(E)** Viable cell percentages, estimated by resazurin oxidation and reduction, for SV40-fibroblasts from a healthy control (C), P1, P1 cells transfected with WT *TRAF3* (P1-WT) and P1 cells transfected with mock vector (P1-mock), 24 hours after infection with VSV, at various multiplicities of infection. The cells were either not treated (left panel), or subjected to prior treatment (right panel) with recombinant IFN-α for 18 hours. **(F)** VSV titers, estimated on Vero cells, in SV40-fibroblasts from a healthy control (C), P1, P1 cells transfected with WT *TRAF3* (P1-WT) or mock vector (P1-mock), at various times after VSV infection, without (left panel) or with (right panel) 18 hours of pretreatment with IFN-α. Mean values ± SD were calculated from three independent experiments.

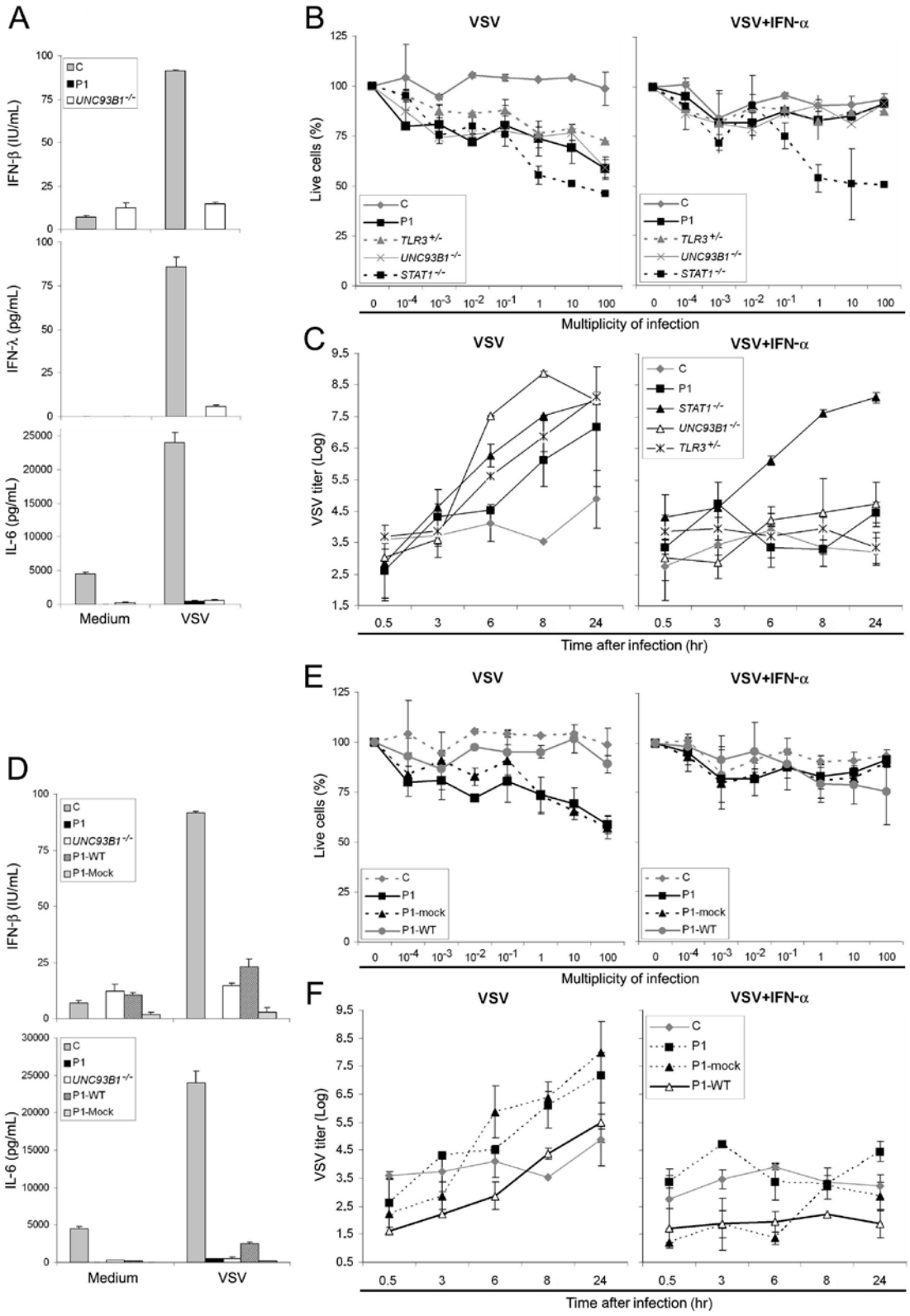
A
IFN-β (IU/mL)
IFN-λ (pg/mL)
IL-6 (pg/mL)
C
P1
UNC93B1-/-
Medium
VSV
B
VSV
VSV+IFN-α
Live cells (%)
C
P1
TLR3+/-
UNC93B1-/-
STAT1-/-
Multiplicity of infection
C
VSV
VSV+IFN-α
VSV titer (Log)
C
P1
STAT1-/-
UNC93B1-/-
TLR3+/-
Time after infection (hr)
D
IFN-β (IU/mL)
IL-6 (pg/mL)
C
P1
UNC93B1-/-
P1-WT
P1-Mock
Medium
VSV
E
VSV
VSV+IFN-α
Live cells (%)
C
P1
P1-mock
P1-WT
Multiplicity of infection
F
VSV
VSV+IFN-α
VSV titer (Log)
C
P1
P1-mock
P1-WT
Time after infection (hr)

Fig. 5. Production of type I IFN and cytokines in immune system cells

(A) Production of IFN-α and IL-12p40 after stimulation with LPS and R-848, as assessed by ELISA, in MDDCs. C is the positive control (one of the eight controls tested) and P1 is patient 1. **(B)** Production of IFN-λ and IL-12p40 after stimulation with LPS and R-848, as assessed by ELISA, in MDMs. C is the positive control (one of the eight controls tested) and P1 is patient 1. **(C)** Production of IFN-β**,** IFN-λ and IL-6, as assessed by ELISA, in SV40-fibroblasts after stimulation with poly(I:C)+Lipofectamine or 7sk-as. C is the positive control and P1 is patient 1; *UNC93B* $^{-/-}$ is an UNC-93B-deficient patient. **(D)** IFN-α production after stimulation with poly(I:C) and various viruses, as assessed by ELISA, in PBMCs. C is the positive control and P1 is patient 1. The panel illustrates results from a single experiment, representative of two. **(E)** Production of IFN-β and IFN-λ, as assessed by ELISA, in SV40-fibroblasts after stimulation with HSV-1. C is the positive control and P1 is patient 1; *UNC93B* $^{-/-}$ is an UNC-93B-deficient patient. Mean values ± SD were calculated from three independent experiments. **(F)** Production of IFN-β and IFN-λ, as assessed by ELISA, in SV40-fibroblasts, after stimulation with various viruses. C is the positive control and P1 is patient 1; *UNC93B* $^{-/-}$*, TLR3* $^{+/-}$ *and MyD88* $^{-/-}$ are patients with the corresponding genotypes.

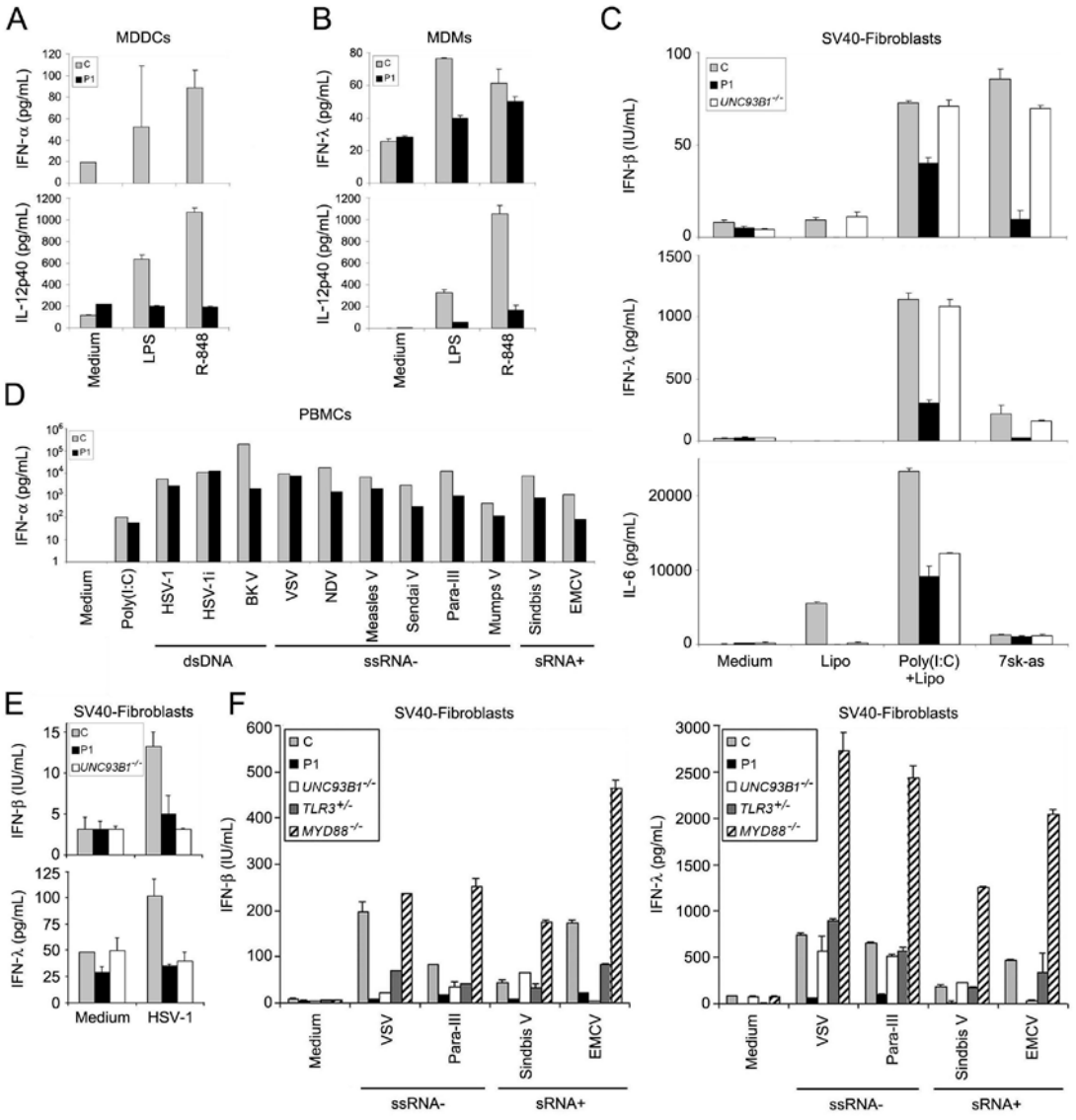
A
MDDCs
IFN-α (pg/mL)
IL-12p40 (pg/mL)
C
P1
Medium
LPS
R-848
B
MDMs
IFN-λ (pg/mL)
C
C
SV40-Fibroblasts
IFN-β (IU/mL)
IFN-λ (pg/mL)
IL-6 (pg/mL)
UNC93B1-/-
Medium
Lipo
Poly(I:C) +Lipo
7sk-as
D
PBMCs
IFN-α (pg/mL)
Medium
Poly(I:C)
HSV-1
HSV-1i
BK V
VSV
NDV
Measles V
Sendai V
Para-III
Mumps V
Sindbis V
EMCV
dsDNA
ssRNA-
sRNA+
E
SV40-Fibroblasts
IFN-β (IU/mL)
IFN-λ (pg/mL)
Medium
HSV-1
F
SV40-Fibroblasts
IFN-β (IU/mL)
TLR3+/-
MYD88-/-
VSV
Para-III
Sindbis V
EMCV
ssRNA-
sRNA+
SV40-Fibroblasts
IFN-λ (pg/mL)

Fig. 6. TRAF3 in TNFR pathways

The production of IL-6 **(A)** and IL-12p40 **(B)** was assessed by ELISA in MDDC, after 24 h of incubation with L-cells transfected with human CD40L (CD40L) and non transfected L-cells (Neg control), for a healthy control (C) and P1. **(C)** Cell death assay, based on resazurin oxidation/reduction, for SV40-fibroblasts from a healthy control (C) and P1 treated with various doses of LTα1β2, with or without IFN-γ (80 IU/ml) for 72 h. **(D)** IL-8 production, assessed by ELISA, in SV40-fibroblasts from control (C), P1, P1 cells transfected with human WT *TRAF3* (P1-WT) or mock vector (P1-mock), after activation with LTα1β2 at the concentration indicated. **(E)** WB analysis of the p52 subunit in EBV-B cells not stimulated (NS) or stimulated with BAFF at a concentration of 100 ng/ml (BAFF). C is the positive control, P1 is patient 1 and *BAFFR* $^{-/-}$ is EBV-B cells from a BAFFR-deficient patient. "Fold induction" indicates densitometry results normalized with respect to GADPH levels, expressed as a fold induction over non stimulated control cells. GADPH was used as an internal control for WB. The panel illustrates results from a single experiment, representative of three. **(F)** IL-10 production, assessed by ELISA, in EBV-B cells, after BAFF activation (100 ng/ml). C is the positive control; P1 is patient 1 and *BAFFR* $^{-/-}$ is a BAFFR-deficient patient. Mean values $\pm$ SD were calculated from three independent experiments.

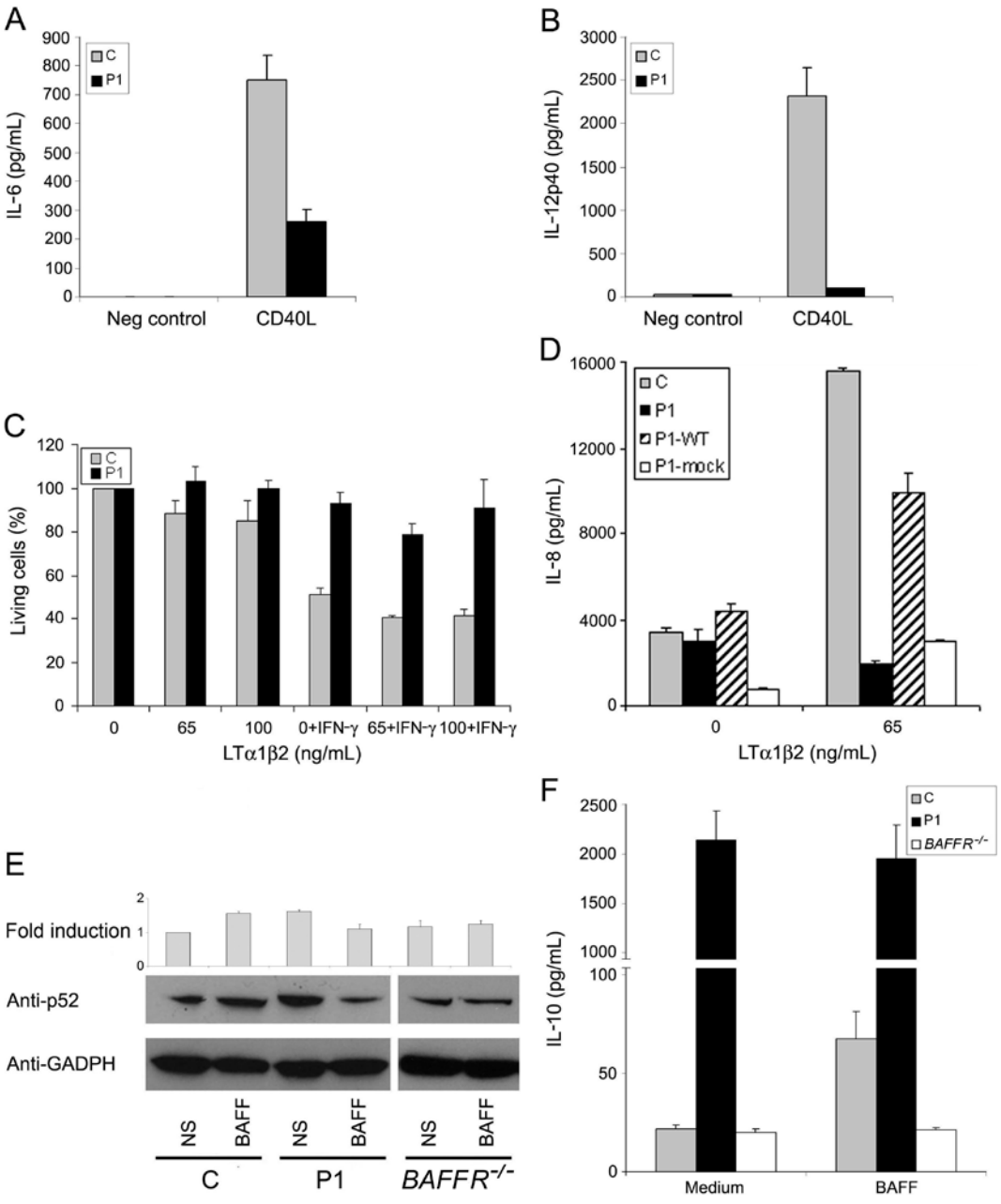
A
IL-6 (pg/mL)
900
800
700
600
500
400
300
200
100
0
C
P1
Neg control
CD40L
B
IL-12p40 (pg/mL)
3000
2500
2000
1500
1000
500
0
C
P1
Neg control
CD40L
C
Living cells (%)
120
100
80
60
40
20
0
C
P1
0
65
100
0+IFN-γ
65+IFN-γ
100+IFN-γ
LTα1β2 (ng/mL)
D
IL-8 (pg/mL)
16000
12000
8000
4000
0
C
P1
P1-WT
P1-mock
0
65
LTα1β2 (ng/mL)
E
Fold induction
2
1
0
Anti-p52
Anti-GADPH
NS
BAFF
NS
BAFF
NS
BAFF
C
P1
BAFFR-/-
F
IL-10 (pg/mL)
2500
2000
1500
1000
100
50
0
C
P1
BAFFR-/-
Medium
BAFF

Supplemental data

SOM Text note 1

Figs. S1 to S6